Check for updates

Extracting lignin from sugarcane bagasse for methylene blue and hexavalent chromium adsorption in textile wastewater: a facile, green, and sustainable approach†

Nhu Y. Nguyen-Thi, [ID] *[a] Cuong Quoc Nguyen, [ID] [b] Quang Le Dang,[c] Quang De Tran, [ID] [b] Tuyet Nhung Do-Thi[a] and Luong Huynh Vu Thanh*[d]

This study presents the process of extracting lignin from sugarcane bagasse collected in the Mekong Delta, Vietnam by the alkali method. NaOH has been used as an effective, environmentally friendly chemical to enhance the extraction process. The obtained lignin was applied for methylene blue (MB) and hexavalent chromium (Cr(VI)) removal. Factors influencing lignin extraction and adsorption processes of MB and Cr(VI) were investigated, showcasing the sustainable reusability of lignin extracted from sugarcane bagasse. Lignin characterization was also carried out by scanning electron microscopy (SEM), Fourier transform infrared spectroscopy (FT-IR) and thermogravimetric analysis (TGA) techniques. The results showed that the extracted lignin content reached 38.61% under optimal conditions (NaOH concentration of 10%, reaction temperature of 90 °C and reaction time of 90 min). The adsorption efficiency and capacity of lignin reached 90.90% and 9.09 mg g^{-1} for MB and 80.10% and 28.04 mg g^{-1} for Cr(VI), respectively, under optimum adsorption conditions (pH, adsorption time, initial methylene blue concentration, and used lignin content). The adsorption process obeyed Langmuir adsorption and was principally physical adsorption. These findings prove sugarcane bagasse based lignin as a cheap and efficient adsorbent for MB and Cr(VI) removal, which contributes to the utilization of the abundant agricultural by-product for wastewater treatment.

1. Introduction

Lignocellulose has gained recognition due to its widespread presence in diverse biomass sources, including agricultural and forest remnants. This characteristic positions it as a compelling contender for viable biorefinery methodologies aimed at sustainability.[1,2] The exploration of lignocellulose's potential offers considerable prospects in mitigating energy and environmental constraints by facilitating biofuel synthesis, the creation of biodegradable substances, and pioneering advancements within the domains of green chemistry and biotechnology. Lignocellulose is composed primarily of three major polymers: lignin, cellulose, and hemicellulose (Fig. 1A).

Lignin provides rigidity and protection, cellulose offers mechanical strength, and hemicellulose contributes to the overall structure.[3] Lignin, a renewable source of aromatic compounds, holds the potential to replace petroleum-derived benzene, toluene, and xylene compounds. So, lignin holds substantial promise as a foundational resource for generating bulk or modified aromatic compounds. Lignin is a natural complex biopolymer structure derived from plants, accounting for 12–39% in plant cells.[3–7] Lignin used to be considered as a pollutant matter for a long time before being used in industrial polymers, chemistry, and environmental engineering. As a phenolic polymer, lignin has been used in a variety of fields like chemical synthesis, medicine, adhesives and environmental treatment.[8–10] The exact structure of lignin currently is a challenge to scientists because it is dependent on plant sources, type of woods, and extraction methods (alkaline methods, ionic liquid method, *etc.*). Basically, lignin is an amorphous heteropolymer consisting of 3 main monomers: coniphenyl alcohol, sinapyl alcohol and *p*-coumaryl alcohol[11] (Fig. 1B and C). Besides the two commercial products of lignin, soft-wood lignin and hard-wood lignin, studies of lignin derived from different sources, namely, grass,[12] rice husk,[13] sugarcane bagasse,[14–17] and coconut fiber[17] were published. The catalytic conversion of

[a] Can Tho University of Technology, Can Tho 94000, Vietnam. E-mail: ntny@ctuet.edu. vn; Tel: +84-909-163-385

[b] Department of Chemistry, College of Natural Sciences, Can Tho University, Can Tho 94000, Vietnam

[c] Institute for Tropical Technology, Vietnam Academy of Science and Technology, Hanoi 10072, Vietnam

[d] Department of Chemical Engineering, College of Engineering, Can Tho University, Can Tho 94000, Vietnam. E-mail: lhvthanh@ctu.edu.vn

† Electronic supplementary information (ESI) available. See DOI: https://doi.org/10.1039/d3ra08007b
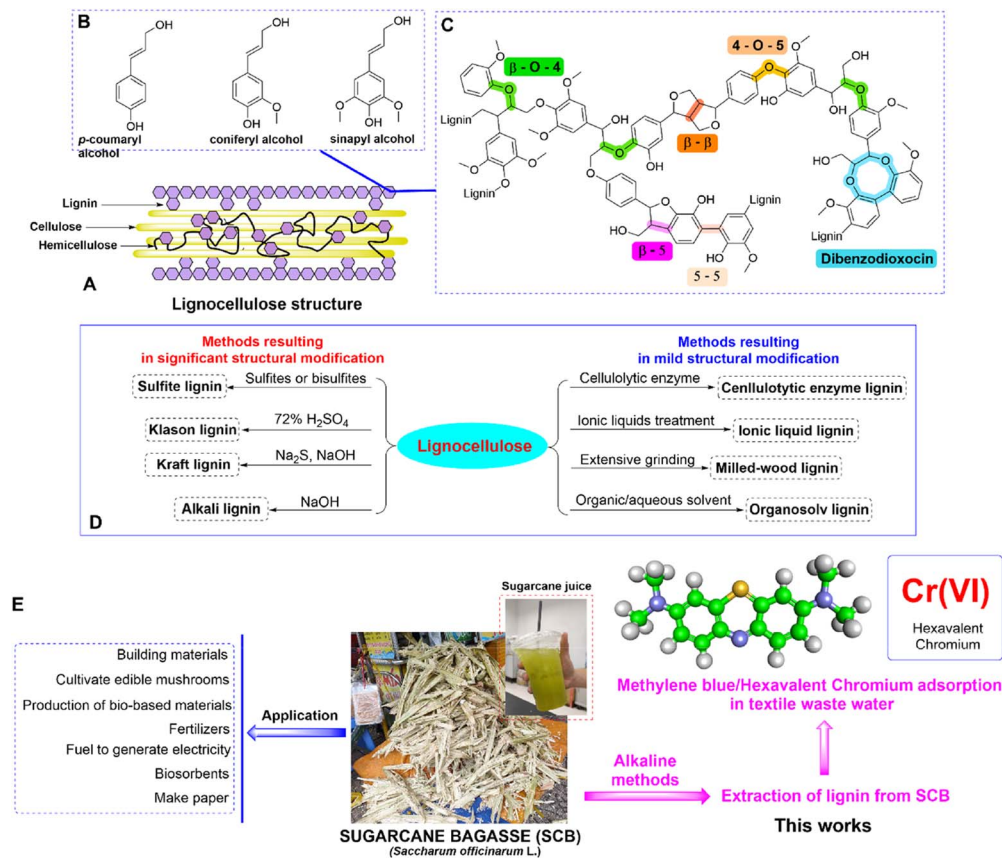
Fig. 1 Representation of the lignocellulose structure (A). Three standard monolignol monomers (B) and a representative lignin structure displaying typical lignin subunits and linkages encountered (C). Some procedures for isolation of lignin from lignocellulose (D). The work is concentrated on the sugarcane bagasse as the biomass raw material of lignin source as an economical and ecologically friendly biosorbent for the efficient removal of MB from textile wastewater (E).

lignin remains an engrossing subject of scientific investigation, promising significant potential for progress (Fig. 1D).

Sugarcane bagasse is an abundant by-product of sugar cane, a major short-term industrial crop in the provinces of the Mekong Delta. Sugarcane bagasse consists mostly of cellulose, accounting for 40–50%, followed by hemicellulose accounting for 20–30%, lignin accounting for 18–25% and a small component of other soluble substances like glucose, sucrose, *etc.* So far, biochar is well-known thanks to its porous structure and high specific surface area, which lead to its excellent potential applications in removal of a variety of inorganic and organic pollutants.[18,19] Some studies on lignin derived from sugarcane bagasse have been conducted for environmental treatment applications.[15–17,20]

Methylene blue (MB) is one of the most common dyes being used in the production processes of textiles, dyeing and printing. These organic dyes are non-biodegradable, mutagenic, toxic and carcinogenic to humans.[21] Therefore, it is necessary to find simple, efficient, and economical methods to treat dye wastewater. Chromium is found in various forms; the primary types include elemental chromium(0), chromium(III), and chromium(VI). Chromium(III) is naturally occurring and plays a crucial role as a nutrient for the human body.[22] On the other hand, chromium(VI) is utilized in textile manufacturing as a catalyst for dyeing and as a dye for wool.[23] It's important to note that hexavalent chromium (Cr(VI)) is marked as a human carcinogen by the International Agency for Research on Cancer (IARC).[24] The use of chromate in textiles and leather tanning can contribute to or worsen contact dermatitis.[24] Many technologies have been applied to treat organic wastewater, such as biological, chemical or physical methods. Among these techniques, adsorption is one of the most favored methods because of its low cost, ease of operation, lower energy consumption, simple setup, high efficiency and non-toxicity.[18,19,21,25]

This study was driven by the central objective of evaluating sugarcane bagasse-derived lignin's viability as an economical and ecologically friendly biosorbent for the efficient removal of MB and Cr(VI) from aqueous solutions (Fig. 1E). The work delved into the intricate interactions between lignin and MB/Cr(VI), with the overarching aim of unveiling a potent solution for pollution remediation by meticulously analyzing the adsorption dynamics and effectiveness of lignin in capturing MB/Cr(VI) molecules. So, the research not only aimed to propose a pragmatic strategy for water decontamination but also aimed to underscore the broader potential of lignin as a versatile resource with multifaceted environmental applications.

2. Experimental

2.1. Materials

Natural biomass resources (sugarcane bagasse, SCB) were collected from Can Tho and Hau Giang, Vietnam (see ESI†). All reagents were purchased from commercial sources and used without further purification. Other chemicals included NaOH (≥98%, pellets (anhydrous), Sigma-Aldrich Inc), H$_2$SO$_4$ (95–98%, Vietnam), methylene blue (≥95%, calc. to the dried substance, Sigma-Aldrich Inc) and deionized water (Vietnam).

2.2. Lignin extraction process

Influencing factors including NaOH solution concentration, reaction temperature, and reaction time were surveyed by the method of alternating each factor to determine the optimal lignin extraction process. First, SCB was chopped into a size of around 1 cm^2 and boiled in distilled water at 70 °C for 2 h to remove sugar. After that, the SCB was dried at 60 °C for 24 h and crushed to approximately 0.5 mm. The crushed SCB was treated with NaOH solution (2–14%) at T (30–120 °C) for t (30–120 min), and then the solid was removed to obtain a black solution. Next, concentrated H$_2$SO$_4$ was slowly added into the black solution to form a yellow precipitant until the solution reached pH 2. Then the precipitate was centrifuged, washed several times with deionized water and dried at 60 °C for 24 h to obtain lignin.

$$\text{Yield of lignin (\%)} = \frac{\text{weight of lignin}}{\text{weight of sugarcane bagasse}} \times 100 \quad (1)$$

2.3. Lignin characterization

The morphology, structural and thermal characterization of lignin was performed by scanning electron microscopy (SEM), Fourier transform infrared spectroscopy (FTIR), and thermogravimetric analysis (TGA). FT-IR measurements were taken using an FT-IR Nicolet 6700 (Thermos). Each scan recorded 50 scans, in the range from 500 to 4000 cm^{-1} with a resolution of 4 cm^{-1}. SEM images of the lignin sample were captured using a Hitachi-TM1000 Tabletop system (Japan). TGA was conducted using a NETZSCH TGA 209 F3 instrument, covering a temperature range of 100 °C to 700 °C, with a heating rate of 10 °C min^{-1}.

2.4. MB adsorption process

The MB adsorption process was examined following the method of alternating each variable to determine the optimal conditions for the whole process. First, a (g) of lignin was added to five 250 mL conical flasks containing 100 mL of b (mg L^{-1}) MB solution. The pH was adjusted from 5 to 9 by using 0.1 N NaOH and 0.1 N HCl solutions, the MB concentration varied from 10 mg L^{-1} to 50 mg L^{-1} in 15–120 min and lignin mass from 5 to 50 mg. The MB concentration after the adsorption process was determined by ultraviolet-visible (UV-vis) measurement after separating the lignin by using a UV-vis/NIR Multiskan SkyHigh (Thermo Fisher).

2.5. Cr(VI) adsorption process

The adsorption process of Cr(VI) was systematically examined similar to the adsorption process of MB. Specifically, a quantity of a (g) of lignin was introduced into each flask containing 100 mL of K$_2$Cr$_2$O$_7$ solution with a concentration of b mg L^{-1}. The pH of the solution was meticulously adjusted within the range of 2.0 to 6.0 using a 0.1 M NaOH and HCl solution. The hexavalent chromium content was determined from the calibration curve at 540 nm to determine the absorbance.

2.6. Kinetic studies

The equilibrium adsorbed concentration, q, and adsorption efficiency, H%, were calculated according to the equations

$$q = \frac{(C_0 - C_e) \times V}{m} \quad (2)$$

$$H = \frac{C_0 - C_e}{C_0} \times 100 \quad (3)$$

where, C_0 (mmol L^{-1}) is the initial MB concentration, C_e (mmol L^{-1}) is the equilibrium concentration in solution, V (L) is the total volume of solution, and m (g) is the lignin mass.

Adsorption kinetics were identified following theoretical pseudo-first-order and pseudo-second-order models. Adsorption isotherms were analyzed according to the Langmuir (eqn (4)) and Freundlich (eqn (5)) models and adsorption type was identified by using the Dubinin–Radushkevich (D–R) model (eqn (6)).

$$\frac{C_e}{q_e} = \frac{1}{q_m K_L} + \frac{C_e}{q_m} \quad (4)$$

$$\ln q_e = \ln K_F + \frac{1}{n} \times \ln C_e \quad (5)$$

where C_e (mg L^{-1}) is the equilibrium concentration of adsorbate, q_e (mg g^{-1}) is the equilibrium adsorption amount, q_m (mg g^{-1}) is the maximum adsorption capacity, K_L (mg^{-1}) is the Langmuir constant, and K_F (mg g^{-1}) and n are the Freundlich constants related to the adsorption capacity and intensity.

$$\ln q_e = \ln q_m - \beta \varepsilon^2 \quad (6)$$

where ε is the Polanyi potential ($\varepsilon = RT \ln(1 + 1/q_e)$, with T being the absolute temperature (K) and R being the universal gas constant), and β is a constant related to the adsorption energy.

3. Results and discussion

3.1. Lignin extraction

Green chemistry represents a progressive paradigm in the realm of chemical science, with its primary emphasis directed toward the advancement of procedures and substances that yield favourable consequences for the environment. The principal focal point of green chemistry revolves around the reduction of detrimental substance employment, the enhancement of production protocols, and the conceptualization of commodities possessing facile recyclability and biodegradability. This

paradigm not only serves environmental interests but also engenders economic and societal dividends. Within the scope of this work, the study endeavour revolves around harnessing agricultural by-products to address the exigencies of contaminated wastewater treatment. This approach adheres to an eco-conscious recycling protocol, circumventing the utilization of organic agents. The environmentally friendly recycling process avoids the use of organic solvents; the primary solvent employed in the research is water.

Fig. 2A displays the lignin extraction process, which was a green and environmentally friendly technique for extraction of lignin. The process was based on the alkali method and the method of alternating each variable was examined. The lignin extraction efficiency is over 38%. In particular, this study shows that it is environmentally friendly and safe for technicians, which is suitable for large-scale production. Previously, lignin preparation studies have been carried out using formic acid, DES, soda/AQ, hydrotropes and organosolv, which required extreme conditions.[26–28] Therefore, these processes are not suitable for the equipment and conditions in Vietnam.

3.1.1. Effect of reaction temperature. The aim of this study is to find a suitable temperature that has a positive effect on the lignin preparation process from the SCB collected in Vietnam. Experiments were conducted at reaction temperatures of 30, 60, 90, and 120 °C, three times for each. Other factors were fixed including 35 g crushed SCB, NaOH 2%, and reaction time of 30 min. The effect of reaction time is presented in Fig. 2B, which showed that increasing reaction temperature led to increasing recovery performance of lignin content. The obtained lignin contents were high at 90 and 120 °C (29.07 and over 30%, respectively). There was a small gap of lignin recovery capacity *versus* a wide gap of energy which supplied temperature.

Besides, the temperature of 120 °C could affect lignin structure. Therefore, 90 °C was chosen as the optimal temperature for the lignin preparation process.

3.1.2. Effect of reaction time. The effect of reaction time on lignin preparation is displayed in Fig. 2C. Reaction times of 30, 60, 90 and 120 min were selected for each experiment. The 35 g crushed SCB was treated with 2% NaOH solution, while the reaction temperature of 90 °C was kept constant. Fig. 2C shows that lignin extraction performance gradually increased and reached the maximum at a reaction time of 90 minutes. In particular, at 120 min, the solution was found to be absolutely heterogeneous mixtures (the lignin content could not be determined), thus leading to a decrease in the efficiency of the process. It would be explained that condensation reaction could take place when the reaction time lasted 120 min due to the appearance of clumps in the solution.

3.1.3. Effect of NaOH concentration. To investigate the influence of NaOH concentration on the lignin preparation process, the study conducted experiments by changing the NaOH concentration. Four different concentrations of sodium hydroxide solution were tested (2, 6, 10, and 14%, respectively), with three times repetition of each experiment. 35 g of crushed SCB was utilized. The optimal reaction temperature and reaction time are 90 °C and 90 min. The effects of NaOH concentration are illustrated in Fig. 2D. Fig. 2D illustrated that with an increase in NaOH concentration, the lignin recovery performance also increased. In this case, NaOH concentration of 10% was selected for next experiments because of the smallest ratio of the yield to used NaOH content got at this level. Furthermore, at the NaOH concentration of 14%, lignin was swollen, causing condensation reaction. This led to difficulties in operation, making the performance decreased.
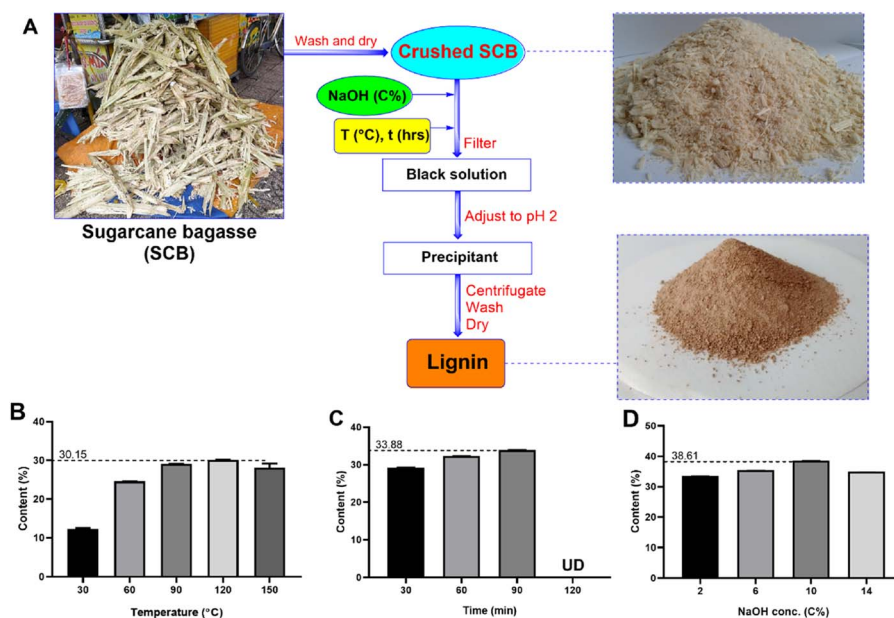

Fig. 2 (A) Schematic illustration of the preparation of lignin from the SCB collected in Vietnam. Effect of temperature (B), time (C), and NaOH concentration (D) on lignin extraction. UD: undeterminable. The bars show mean ± SD. The experiments were repeated three times with similar results.

3.2. Lignin characterization

For structural confirmation of prepared lignin, thermogravimetric analysis (TGA), scanning electron microscopy (SEM) and FTIR analysis were performed. SEM analysis showed that lignin particles were in the shape of a polyhedron (Fig. 3A). The size of particles distributed in a wide range from 0.1 to 2.0 μm. Based on this fact, it can be concluded that extracted lignin presents an adequate morphology for hydrophobic constituent adsorption. Infrared spectroscopy is currently one of the important analytical techniques available to analyze almost any type of sample. The FTIR spectra are presented in Fig. 3B. The presence of characteristic peaks in FTIR spectra indicates the presence of lignin on the sample, such as the peaks centered at 3393 cm^{-1} (phenolic and aliphatic –OH), 2923 cm^{-1} (C–H stretching), 1710 cm^{-1} (C=O stretching vibration of ester, carbonyl and non-conjugated ketone), 1515 cm^{-1} (C–C aromatic skeleton), 1460 cm^{-1} (C–H asymmetry), 1246 cm^{-1} (C–C guaiacyl aromatic ring), 1000–1150 cm^{-1} (strength vibration of C–OH side groups and the C–O–C glycosidic), and 831 cm^{-1} (–CH bending in aromatic ring). The data from the FTIR spectroscopy show agreement and similarity with the recently published results for lignin prepared from agricultural by-products and wastes.[29,30] Thermogravimetric analysis was performed from room temperature to 700 °C (Fig. 3C and see ESI†). The TGA curve presented that thermal degradation of lignin could be divided into 4 temperature ranges of 30–700 °C. Range I (30–140 °C) is related to moisture in lignin particles. There are very few peaks occurring in the range of 180–250 °C. This proved that lignin particles contained very little hemicellulose content. The results showed that lignin degradation took place slowly over a wide temperature range. The decomposition took place fastest at 280–370 °C. This could be explained by the complex structure of lignin with phenolic, carbonyl, and benzylic hydroxyl groups linked together. Char and coke were made at high temperature (range IV).

3.3. Identification of the point of zero charge (PZC)

The PZC graph showed that pH$_{pzc}$ was 4.4 (Fig. 3D). This indicates that in a solution with pH < pH$_{pzc}$, H$^+$ is predominant, making the surface of the adsorbent material carry a positive charge, resulting in better anion adsorption. Similarly, when solution pH is higher than pH$_{pzc}$, the surface of the material has a negative charge and the ability to adsorb cations will be better.

3.4. Removal of MB using lignin

3.4.1. Effect of pH. The pH plays a crucial role in adsorption capacity because pH affects not only the surface charge of the adsorbent, but also the degree of ionization due to the reacting dye molecule. To evaluate the influence of pH on the MB adsorption capacity of bagasse derived lignin, different pH conditions ranging from 5.0 to 9.0 were studied, and the initial MB concentration of 20 mg L^{-1} was fixed (Fig. 4A).

In general, the MB adsorption efficiency of lignin was relatively high (above 75%). The adsorption efficiency increased from over 75% at pH 5 to over 90% at pH 6. This was consistent with zero-point charge analysis. This could be explained by competitive adsorption. pH 5 caused a competitive adsorption of H$^+$ ions with MB$^+$ cations, leading to low MB adsorption efficiency. At pH 6, H$^+$ gradually decreased and was replaced by OH$^-$, and competitive adsorption decreased. Therefore, the adsorption efficiency was higher. However, the adsorption efficiency decreased when the pH was higher than 6, and the reduction was considered insignificant, which could be explained by the lignin solubility in alkaline. Therefore, pH 6 with the highest adsorption efficiency and adsorption capacity was chosen for next surveys.

3.4.2. Effect of adsorption time. Effect of adsorption time was determined, as shown in Fig. 4B. The results showed that the adsorption efficiency and adsorption capacity increased to the highest point at 60 min, and almost remained stable after that, so the optimal adsorption time of 60 min was selected.

3.4.3. Effect of lignin content. In contrast to adsorption efficiency, the adsorption capacity gradually decreased from 8.91 to 1.98 mg g^{-1} when the lignin content increased from 0.2 to 1.0 g (Fig. 4C). This proved that the initial lignin content was regularly sufficient for the adsorption process. Therefore, adsorption capacity increased insignificantly when the adsorbent content was continuously increased. It is necessary to use the appropriate amount of lignin to limit adsorbent material waste, so a lignin content of 0.2 g was chosen.

3.4.4. Effect of MB concentration. The influences of MB concentration are shown in Fig. 4D. The adsorption efficiency reached over 95% when the MB concentration was 10 mg L^{-1}. When the MB concentration increased from 10 to 50 mg L^{-1}, the adsorption efficiency decreased. This could be explained as follows: when the concentration of MB was low, the MB$^+$ cations moved freely, so the lignin easily combined to most of the MB$^+$ cations in the solution. The change in MB adsorption capacity of lignin was opposite to the adsorption efficiency; when MB concentration increased, the adsorption capacity increased. This could be explained that when MB$^+$ concentration increased, which means that the amount of available MB$^+$ was
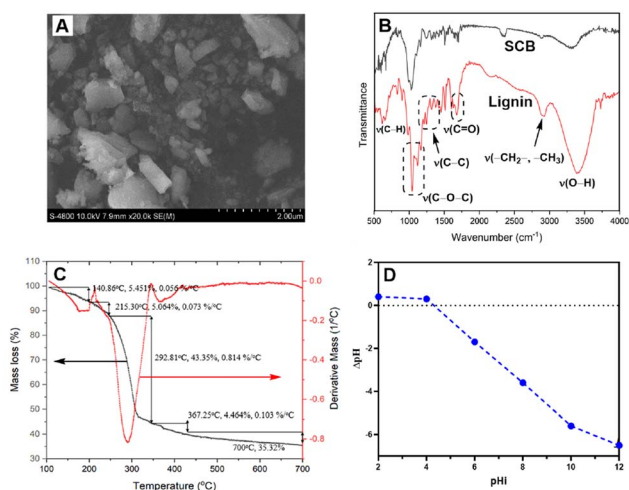

Fig. 3 SEM image (A), FTIR spectra (B), TGA plot (C) and pH$_{pzc}$ plot (D) of SCB-based lignin (SCB: sugarcane bagasse).
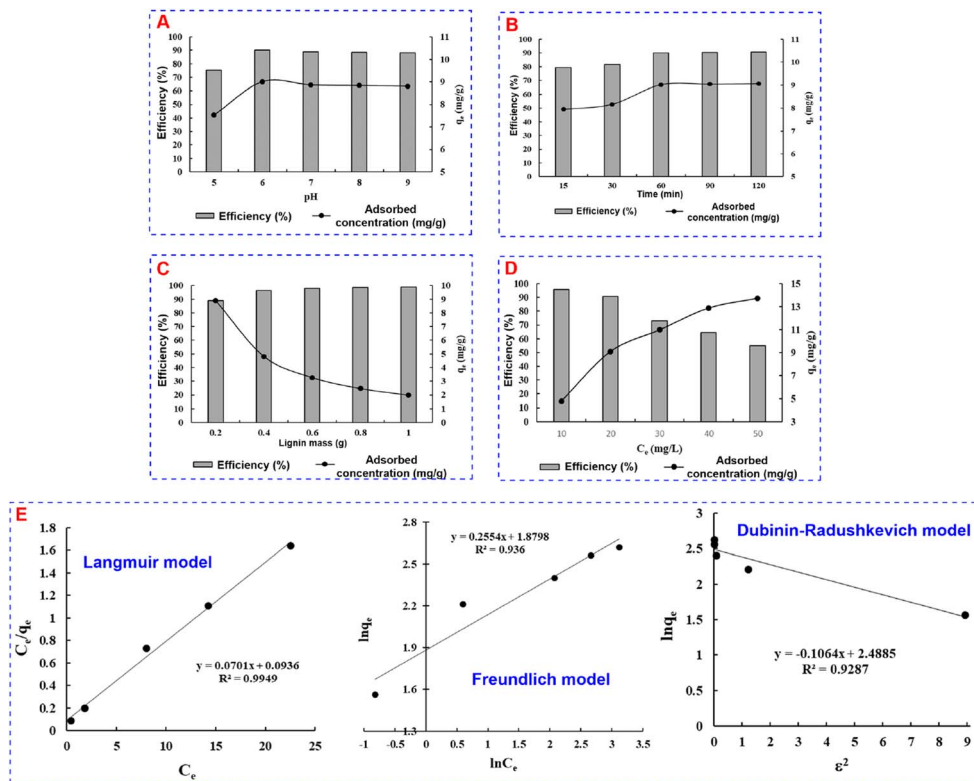
Fig. 4 Optimal parameters for MB adsorption utilizing lignin derived from SCB. Effect of pH (A), adsorption time (B), lignin content (C), and MB concentration (D). MB adsorption isotherms of SCB-based lignin (E).

high, lignin could adsorb more MB, so the adsorption capacity increased gradually through each concentration level investigated. Therefore, a MB concentration of 20 mg L^{-1} was chosen as the optimal concentration because both adsorption efficiency and adsorption capacity are not too low.

3.4.5. Kinetics and isotherm of MB adsorption. It is crucial to determine the kinetic models to clarify the adsorption mechanism of the adsorbent. Kinetic models and the corresponding parameters are shown in Fig. 4E.

The MB kinetic model parameters of lignin following the hypothetical adsorption models are shown in Table 1. In the first-order hypothetical equation, the correlation coefficient showed a high consistency between the parameters with the monolayer adsorption of MB on the surface of lignin material ($R^2 = 0.9949$), corresponding to maximum adsorption capacity, q_m, 14.26 mg g^{-1}. In the second-order hypothetical equation, the correlation coefficient R^2 of 0.936 indicated that the adsorption process occurred partly due to the weak binding forces between the adsorbent and the adsorbate. This

confirmed that the MB adsorption onto lignin followed the first-order adsorption kinetics and Langmuir isotherm model.

To determine whether the nature of MB adsorption is physical or chemical adsorption, the D–R isotherm model was applied. The D–R model and parameters are presented in Fig. 3E and Table 2. The average adsorption energy E of 2.17 kJ mol^{-1} (<8 kJ mol^{-1}) indicated that the MB adsorption process of lignin was a physical adsorption process.[31,32] However, a correlation coefficient R^2 of 0.9287 is not too high; this could be a little comparative chemical adsorption taking place parallelly along with physical adsorption.

MB adsorption capacity for each material has different values. This study contributes a new type of adsorbent originating from local farming for methylene blue removal.

3.5. Removal of Cr(vi) using lignin

3.5.1. Effect of pH. The adsorption efficiency of Cr(vi) by lignin is observed to be relatively modest overall (Fig. 5A),

Table 1 Adsorption kinetic model parameters

	Pseudo first order			Pseudo second order		
	q_m (mg g^{-1})	K_L (gm^3 mg^{-1})	R^2	$1/n$	K_F ((mg g^{-1}) (dm^3 mg^{-1})$^{1/n}$)	R^2
MB adsorption	14.26	0.75	0.9949	0.255	75.82	0.9360
Cr(vi) adsorption	35.27	0.28	0.9989	0.1329	982.36	0.9072

Paper

RSC Advances

Table 2 Dubinin–Radushkevich parameters

	q_m (mg g^{-1})	R^2	B (mol^2 J^{-2S})	E (kJ mol^{-1})
MB adsorption	12.04	0.9287	0.1046	2.17
Cr(VI) adsorption	32.95	0.9467	5.6528	0.30

showing an increasing trend as the pH increases from 2 to 3 (61.57% to 64.31%), followed by a gradual decrease as the pH continues to rise. This observed variability in adsorption efficiency with increasing pH can be elucidated by considering the initial acidic conditions (pH 2 and 3), where the predominant adsorption environment is acidic (H$^+$ ions prevail), fostering competitive adsorption within the solution. The competitive interaction between H$^+$ and Cr(VI) ions depends on the calculated pH$_{pzc}$ results (see ESI†). It is discerned that at pH levels below pH$_{pzc}$, a heightened inclination towards Cr(VI) adsorption is manifested, resulting in significantly augmented adsorption efficiency compared to pH 4, 5, and 6. As the pH increases, a competitive interplay for adsorption ensues among H$^+$, OH$^-$, and Cr(VI), with a pronounced predilection for OH$^-$, precipitating a diminution in adsorption efficiency. The dissociation of Cr(VI) in solution displayed that the pH range from 2 to 5 corresponds to the prevailing presence of Cr(VI) in the forms of HCrO$_4^-$ and partially Cr$_2$O$_7^{2-}$ (see ESI†). This dual presence creates an amenable milieu for adsorption, primarily facilitated by the prevalence of HCrO$_4^-$. However, as the pH exceeds 5, the

conversion of HCrO$_4^-$ to CrO$_4^{2-}$, a less amenable form for adsorption, results in a noticeable disparagement in adsorption efficiency between pH 6 and lower pH values. The adsorption capacity exhibits a progressive increase with increasing pH, culminating in its maximum at 32.16 mg g^{-1} at pH 3. Subsequently, a diminishing adsorption capacity is discerned with increasing pH, reaching its minimum at 18.19 mg g^{-1} at pH 6. This dynamic shift underscores the substantive impact of pH on the Cr(VI) adsorption capacity of lignin. Consequently, pH 4 emerges as the optimal pH for the adsorption of Cr(VI), and acidic condition ensures that lignin is not dissolved back.

3.5.2. Effect of adsorption time. The temporal aspect is also recognised as a critical determinant influencing the adsorption efficacy of lignin toward Cr(VI). Consequently, a series of experiments were conducted on the adsorption behaviour under constant lignin dosage within a uniform volume of K$_2$Cr$_2$O$_7$ solution at a fixed concentration, spanning discrete durations of 15, 30, 60, 90, and 120 minutes. The results, as depicted in Fig. 5B, reveal a gradual increase in adsorption efficiency as the adsorption duration extends, progressing from 61% to over 65%. This suggests that temporal adjustments exert a negligible impact on the Cr(VI) adsorption capacity of lignin. When the adsorption time was around 60 minutes, the Cr(VI) adsorption capacity was over 65%, and thereafter, changes became negligible. This observation implies that a 60 minutes contact period adequately facilitates the interaction between lignin and Cr(VI), achieving nearly complete adsorption equilibrium.
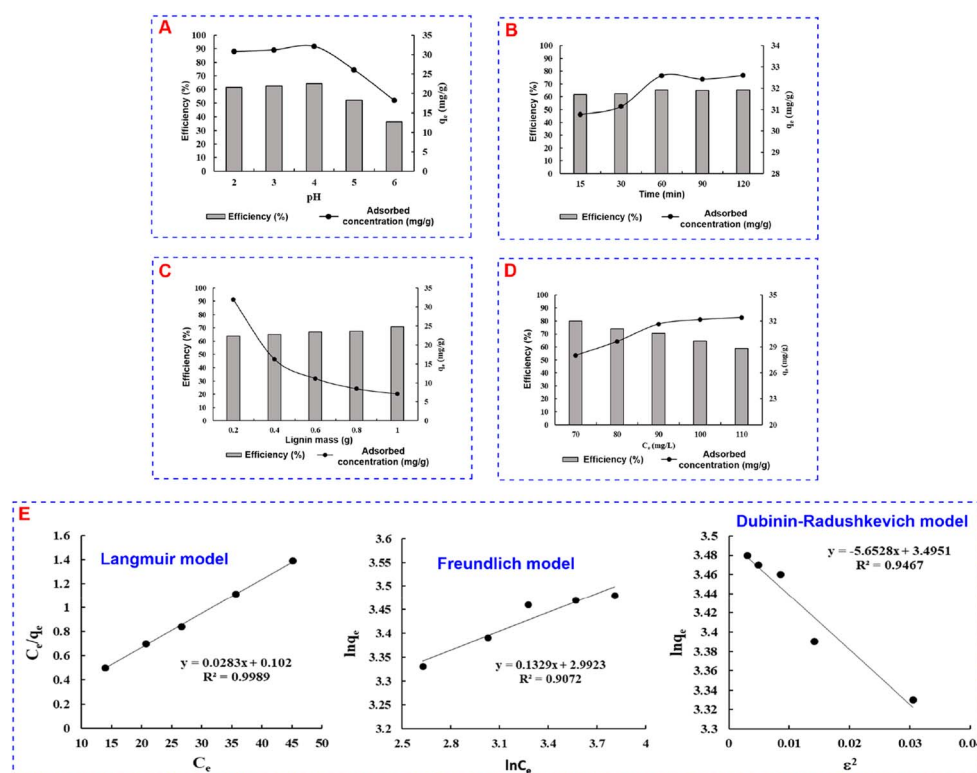

Fig. 5 Optimal parameters for Cr(VI) adsorption utilizing lignin derived from SCB. Effect of pH (A), adsorption time (B), lignin content (C), and Cr(VI) concentration (D). Cr(VI) adsorption isotherms of SCB-based lignin (E).

Likewise, the adsorption capacity exhibits a progressive increase from 30.77 mg g^{-1} to 31.14 mg g^{-1} and further to 32.59 mg g^{-1} at 15, 30, and 60 minutes, respectively. Beyond this interval, a plateau in adsorption capacity at 90 and 120 minutes signifies that the lignin surface approaches saturation. Thus, after 60 minutes of adsorption, the process was deemed nearly complete and no further extensions in time resulted in a significant improvement in adsorption capacity.

3.5.3. Effect of lignin content. The investigation aimed to elucidate the impact of varying the quantities of lignin (0.2, 0.4, 0.6, 0.8, and 1.0 g) on the adsorption capacity of Cr(vi). The efficiency of Cr(vi) adsorption by lignin exhibits a progressive increase, rising from 63% to over 70% as the lignin mass varies. Fig. 5C reveals that the performance disparities among the examined quantities are relatively modest. With an increase in the lignin mass, the adsorption capacity experiences a discernible decline, from 31.91 mg g^{-1} to 7.08 mg g^{-1}. The substantial difference underscores the significant impact of varying the quantity of the adsorbent material on the adsorption capacity. Initially, even with a minimal quantity of lignin, the adsorption capacity attains 31.91 mg g^{-1}. However, as the amount of material increases to 0.4 g, the adsorption capacity undergoes a reduction of nearly 50%, settling at 16.28 mg g^{-1}. This phenomenon can be rationalised by the initial constraint in the amount of adsorbent material, facilitating effective contact between metal ions and the majority of the lignin. Additionally, the occurrence of multi-layered adsorption during the adsorption process contributes to the initial heightened adsorption capacity. Consequently, for the judicious selection of an optimal lignin mass for Cr(vi) adsorption, 0.2 g emerges as the pragmatic choice for this study. This quantity strikes a balance between utilising a moderate amount of lignin and achieving a commendable adsorption capacity.

3.5.4. Effect of Cr(vi) concentration. According to the findings presented in Fig. 5D, the adsorption efficiency shows a gradual decline, from 80.10% to 58.92%, with a progressive elevation in Cr(vi) concentration (from 70 to 110 mg L^{-1}). This observation underscores the pronounced influence of concentration fluctuations on the adsorption capability of lignin. Lignin demonstrates prompt and effective adsorption even at the initial concentration, where molecular interstices allow successive adsorption of Cr(vi) ions onto the lignin surface. However, as the Cr(vi) concentration increases within a constant volume, the restricted mobility between these metal ions curtails their contact with the material, resulting in a concomitant reduction in the adsorption efficiency.

On the contrary, the adsorption capacity displays more subdued variability, showing a gradual increase as the adsorption concentration augments. The maximum in adsorption capacity is observed at a concentration of 110 mg L^{-1} (q_e = 32.41 mg g^{-1}), while the minimum is observed at 70 mg L^{-1} (q_e = 28.04 mg g^{-1}). From the start, lignin manifests a relatively robust adsorption capacity across the investigated concentration, suggesting substantial surface occupancy by adsorbed species. When the concentration reaches 100 mg L^{-1}, almost complete adsorption has transpired. Consequently, further escalation to 110 mg L^{-1} induces

marginal changes in adsorption capacity. In light of these analyses, a concentration of Cr(vi) solution of 100 mg L^{-1} is deemed optimal for adsorption, as it aligns with both a relatively high adsorption efficiency and a stable adsorption capacity.

3.5.5. Kinetics and isotherm of Cr(vi) adsorption. The Langmuir adsorption isotherm model postulates a homogeneous adsorption scenario for Cr(vi) ions on the material surface, presuming a monolayer adsorption without interactions between the adsorbed ions. The linear form of the Langmuir isotherm equation is represented in Fig. 5E. The exceptionally high R^2 value of 0.9989 attests to the robustness of the Langmuir isotherm in describing the adsorption of Cr(vi) by lignin. As displayed in Table 1, the Cr(vi) adsorption capacity by lignin reaches q_m = 35.27 mg g^{-1}, which indicates complete monolayer adsorption on the material surface. Contrastingly, the Freundlich isotherm delineates heterogeneous adsorption during the Cr(vi) adsorption process by lignin, evident through the $1/n$ value being less than 1. The equation manifests a good fit with the R^2 value of 0.9072. In terms of fitting the Cr(vi) adsorption process by lignin, the data from Table 1 show that the Langmuir isotherm has a higher R^2 value, indicating a better suitability. This implies that each adsorption site predominantly accommodates a fraction of the adsorbate, essentially fostering monolayer adsorption on the material surface. The linearised equation of the D–R isotherm model and the data compiled in Table 2 and illustrated in Fig. 5E substantiate that the Cr(vi) adsorption process by lignin aligns with a physical adsorption mechanism. This conclusion is drawn from the E value being 0.3 kJ mol^{-1}, significantly below the typical threshold of 8 kJ mol^{-1} for chemical adsorption.

3.6. Recycling test

Lignin regeneration was systematically conducted up to six times, as represented in similar previous research.[33] The results are depicted in Fig. 6. In the first two runs, the removal efficiency exhibited remarkable performance, achieving over 99% and over 98%, respectively. However, as the process continued, a gradual decline was observed, with the removal efficiency
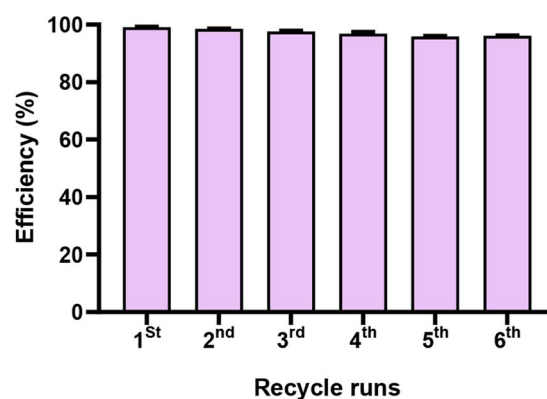
Fig. 6 The regeneration performance of the lignin sourced from sugarcane bagasse. Values are shown after two independent tests (±SD).

slightly diminishing to 95% and 96% in the fifth and sixth iterations, respectively. In another recent study, coal-based activated carbons from three types of long-flame coals with varying ash and volatile matter content were prepared for efficient regeneration, yielding a consistent over 98% MB removal efficiency after five cycles.[33]

In summary, this finding underscores the significant economic advantage associated with the utilization of lignin sourced from sugarcane bagasse for the elimination of harmful dyes, as exemplified in this research with MB as the model pollutant. It emphasizes the cost-effectiveness and sustainability of lignin-based treatment methods, highlighting their potential for addressing environmental and industrial challenges related to dye removal.

4. Conclusions

Our research successfully extracted lignin from sugarcane bagasse, a by-product in the Mekong Delta, Vietnam, and applied it to MB and Cr(VI) adsorption. In this study, lignin was observed to be polyhedron particles in shape and micro particles in size. Optimal conditions for the lignin separation process and MB/Cr(VI) adsorption were determined. NaOH has been used in several studies as an effective, environmentally friendly chemical to enhance the extraction of lignin. Lignin extracted from bagasse gave a MB adsorption efficiency of 90.09% and Cr(VI) adsorption efficiency of 80.10% according to Langmuir adsorption and physical adsorption models. With such a high adsorption capacity, facile and cost-effective method, lignin could be an efficient adsorbent for removal of heavy metal, inorganic and organic pollutants.

Author contributions

N. Y. N. T.: project administration, supervision, and writing – review and editing; C. Q. N.: data curation, designing, and writing – original draft; Q. L. D.: methodology; Q. D. T.: methodology; T. N. D. T.: review and editing; L. H. V. T.: project administration. All authors have reviewed and approved the final draft.

Conflicts of interest

There are no conflicts to declare.

Acknowledgements

References

1 Y. K. Nandabalan, M. U. T. Mohamed, S. Sachdeva and S. Thakur, *Fermentation*, 2023, **9**, 238.

2 Z. Gao, K. Alshehri, Y. Li, H. Qian, D. Sapsford, P. Cleall and M. Harbottle, *Renewable Sustainable Energy Rev.*, 2022, **170**, 112995.

3 M. Mariana, T. Alfatah, A. K. HPS, E. B. Yahya, N. Olaiya, A. Nuryawan, E. Mistar, C. Abdullah, S. Abdulmadjid and H. Ismail, *J. Mater. Res. Technol.*, 2021, **15**, 2287–2316.

4 A. Duval and M. Lawoko, *React. Funct. Polym.*, 2014, **85**, 78–96.

5 S.-J. Jung, S.-H. Kim and I.-M. Chung, *Biomass Bioenergy*, 2015, **83**, 322–327.

6 J. C. Carvajal, Á. Gómez and C. A. Cardona, *Bioresour. Technol.*, 2016, **214**, 468–476.

7 S. Al Arni, *Ind. Crops Prod.*, 2018, **115**, 330–339.

8 M. Vinardell, V. Ugartondo and M. Mitjans, *Ind. Crops Prod.*, 2008, **27**, 220–223.

9 P. Carrott and M. R. Carrott, *Bioresour. Technol.*, 2007, **98**, 2301–2312.

10 D. Stewart, *Ind. Crops Prod.*, 2008, **27**, 202–207.

11 D. A. Baker, N. C. Gallego and F. S. Baker, *J. Appl. Polym. Sci.*, 2012, **124**, 227–234.

12 P. Mousavioun and W. O. Doherty, *Ind. Crops Prod.*, 2010, **31**, 52–58.

13 S. H. Ghaffar and M. Fan, *Biomass Bioenergy*, 2013, **57**, 264–279.

14 S. Jose, L. Mishra, G. Basu and A. Kumar Samanta, *J. Nat. Fibers*, 2017, **14**, 510–518.

15 J. C. del Río, A. G. Lino, J. L. Colodette, C. F. Lima, A. Gutiérrez, Á. T. Martínez, F. Lu, J. Ralph and J. Rencoret, *Biomass Bioenergy*, 2015, **81**, 322–338.

16 H. D. Utomo, R. Y. N. Phoon, Z. Shen, L. H. Ng and Z. B. Lim, *Nat. Resour.*, 2015, **6**, 209.

17 M. Brienzo, W. Carvalho and A. M. Milagres, *Appl. Biochem. Biotechnol.*, 2010, **162**, 1195–1205.

18 K. Wang, Y. Wang, S. Zhang, R. Wang and S.-H. Ho, *Environ. Sci. Ecotechnology*, 2022, **10**, 100168.

19 M. Du, Y. Zhang, Z. Wang, M. Lv, A. Tang, Y. Yu, X. Qu, Z. Chen, Q. Wen and A. Li, *Chem. Eng. J.*, 2022, **442**, 136147.

20 T. C. Andrade Siqueira, I. Zanette da Silva, A. J. Rubio, R. Bergamasco, F. Gasparotto, E. Aparecida de Souza Paccola and N. Ueda Yamaguchi, *Int. J. Environ. Res. Public Health*, 2020, **17**, 526.

21 M. Mohammed, A. Shitu and A. Ibrahim, *Res. j. chem. sci.*, 2014, **2231**, 606X.

22 *Office of Dietary Supplements – Chromium*, https://ods.od.nih.gov/factsheets/Chromium-HealthProfessional/, accessed October 1, 2023.

23 *Chromium in fabrics*, https://oecotextiles.blog/2013/02/28/chromium-in-fabrics/, accessed October 2, 2023.

24 J. P. Wise, J. L. Young, J. Cai and L. Cai, *Environ. Int.*, 2022, **158**, 106877.

25 N. Kannan and M. M. Sundaram, *Dyes Pigm.*, 2001, **51**, 25–40.

26 D. Watkins, M. Nuruddin, M. Hosur, A. Tcherbi-Narteh and S. Jeelani, *J. Mater. Res. Technol.*, 2015, **4**, 26–32.

27 D. Tian, R. P. Chandra, J.-S. Lee, C. Lu and J. N. Saddler, *Biotechnol. Biofuels*, 2017, **10**, 1–10.

28 T. Yimtrakarn, W. Kaveevivitchai, W.-C. Lee and N. Lerkkasemsan, *Polymers*, 2022, **14**, 814.

29 R. Md Salim, J. Asik and M. S. Sarjadi, *Wood Sci. Technol.*, 2021, **55**, 295–313.

30 R. Nandanwar, A. Haldar, A. Chaudhari and J. Ekhe, *J. Chem., Biol. Phys. Sci.*, 2016, **666**, 958–969.

31 A. Kangmennaa, S. Acquah, R. B. Forkuo, J. K. Adusei, G. A. Atongo, F. A. Amarh, F. Opoku and E. S. Agorku, *J. Dispersion Sci. Technol.*, 2024, 1–14.

32 N. Hasani, T. Selimi, A. Mele, V. Thaçi, J. Halili, A. Berisha and M. Sadiku, *Molecules*, 2022, **27**, 1856.

33 T. Niu, J. Zhou, C. Zhang and S. Li, *RSC Adv.*, 2018, **8**, 26978–26986.